Muscle arm development in *Caenorhabditis elegans*

Scott J. Dixon and Peter J. Roy*

Department of Medical Genetics and Microbiology, Collaborative Program in Developmental Biology, University of Toronto, Toronto, ON, M5S 1A8, Canada

*Author for correspondence (e-mail: peter.roy@utoronto.ca)

Accepted 22 April 2005

Development 132, 3079-3092
Published by The Company of Biologists 2005
doi:10.1242/dev.01883

Summary

In several types of animals, muscle cells use membrane extensions to contact motor axons during development. To better understand the process of membrane extension in muscle cells, we investigated the development of *Caenorhabditis elegans* muscle arms, which extend to motor axons and form the postsynaptic element of the neuromuscular junction. We found that muscle arm development is a highly regulated process: the number of muscle arms extended by each muscle, the shape of the muscle arms and the path taken by the muscle arms to reach the motor axons are largely stereotypical. We also investigated the role of several cytoskeletal components and regulators during arm development, and found that tropomyosin (LEV-11), the actin depolymerizing activity of ADF/cofilin (UNC-60B) and, surprisingly, myosin heavy chain B (UNC-54) are each required for muscle arm extension. This is the first evidence that UNC-54, which is found in thick filaments of sarcomeres, can also play a role in membrane extension. The muscle arm phenotypes produced when these genes are mutated support a 'two-phase' model that distinguishes passive muscle arm development in embryogenesis from active muscle arm extension during larval development.

Key words: Muscle arms, Membrane extension, Myosin, actin, ADF/cofilin, Tropomyosin, *unc-54*, *lev-11*, *unc-60*, *Caenorhabditis elegans*

Introduction

The ability of a cell to extend membrane is essential for numerous processes throughout animal development. For example, neurons extend axons and dendrites to establish contact and exchange information between distantly located cells. Recently it has been shown that postmitotic striated muscle cells also extend membrane in a regulated fashion. During the development of the neuromuscular junction, muscles use specialized filopodia to contact incoming motor axons. This was first observed in *Drosophila*, in which actin-filled muscle membrane extensions, called myopodia, cluster at sites of motor axon innervation during embryonic development (Ritzenthaler et al., 2000). The term 'myopodia' has since been adopted by others to describe the membrane extensions that emanate from embryonic mouse skeletal muscle myotubes and make contact with incoming motor axons (Misgeld et al., 2002). Muscle membrane extension may be a common feature of mammalian skeletal muscle cells, as cultured rat myotubes also extend 'micro-spikes' at sites of motoneuron apposition (Uhm et al., 2001). In all three cases, muscle membrane extensions disappear after the neuromuscular junction has formed, suggesting that these extensions have specific roles in guiding or stabilizing incoming motor axons during development. However, it is unknown if the development of muscle membrane extensions in *Drosophila*, mice and rats is controlled by similar mechanisms. Nevertheless, these observations suggest that membrane extension is developmentally regulated in muscle cells. To better understand muscle membrane extensions we have begun to study an analogous process in the nematode worm *Caenorhabditis elegans*.

Adult *C. elegans* have 95 body wall muscles (BWMs) that are required for locomotion and movement of the head. These muscle cells are arranged in four quadrants along the length of the animal (Fig. 1). The two dorsal quadrants flank the dorsal cord, while the two ventral quadrants flank the ventral cord. Within each quadrant there are two longitudinal rows of muscle cells, a proximal row close to the nerve cord, and a distal row further from the cord that we refer to as distal BWMs. The BWMs of nematodes establish contact with motor axons using specialized membrane extensions called muscle arms (Stretton, 1976; Sulston and Horvitz, 1977; Sulston et al., 1983; White et al., 1986). Muscle arms have a simple morphology consisting of a thin stalk that emanates from the cell body and a bifurcated terminus that contacts the nerve cord. The 16 anteriormost BWMs in the head extend muscle arms exclusively to motor axons in the nerve ring (Fig. 1). Immediately posterior to the head muscles, 16 neck BWMs extend arms both to the nerve ring and to the nearest nerve cord. The remaining 63 BWMs extend muscle arms exclusively to motoneurons located in the nearest nerve cord. By contrast to the muscle membrane extensions observed during neuromuscular junction formation in *Drosophila*, rat and mouse, *C. elegans* muscle arms are maintained throughout the life of the animal.

How muscle arms reach the nerve cord is not clear. However, two lines of evidence suggest that a chemoattractant guides the migration of muscle arms to the nerve cords. First, muscle arms extend to motor axons irrespective of their physical position.

For example, commissural motor axons in *unc-6/netrin* or *unc-5/RCM* mutants do not complete their ventral-to-dorsal migrations and instead migrate along the longitudinal axis at sublateral positions. In these mutants, the dorsal BWM arms that normally extend to the motoneurons of the dorsal cord instead extend to the errant lateral motor axons (Hedgecock et al., 1990). Second, muscle arms extend to locations of dense core vesicle accumulation in the cell bodies of motoneurons in *unc-104* mutants (Hall and Hedgecock, 1991; Zhou et al., 2001). This observation suggests that the dense core vesicles contain a muscle arm chemoattractant. *unc-104* encodes a kinesin motor protein that is required for anterograde transport of vesicles within axons (Hall and Hedgecock, 1991; Zhou et al., 2001). These two lines of evidence suggest that muscle arm migration to the nerve cords may be analogous to axon extension toward the source of a chemoattractive cue.

Membrane extension is a conserved process that has been studied extensively in vitro and to a more limited extent in vivo. Membrane extension is normally inhibited by capping actin filaments at the barbed end, which prevents filament elongation (Pollard and Borisy, 2003). However, local activation of ADF/cofilin at the leading edge can sever actin filaments and generate exposed barbed ends (DesMarais et al., 2004; Ghosh et al., 2004). F-actin elongation can then be initiated from these newly exposed barbed ends and provide the force necessary for membrane protrusion. Furthermore, the incorporation of G-actin-ATP monomers on to newly exposed barbed ends results in ATP-rich actin filaments that are the preferred sites of Arp2/3-mediated actin side-branching (Ichetovkin et al., 2002). Extensive Arp2/3-mediated filament side-branching results in a 'dendritic array' actin network at the leading edge that supports the protrusion of a broad lamellae (Svitkina et al., 1997). In regions posterior to the leading edge, tropomyosin binds actin filaments, suppressing Arp2/3-mediated side branching and protecting actin filaments from ADF/cofilin-mediated severing and disassembly (DesMarais et al., 2002; Ono and Ono, 2002). Many of these proteins are required for the development of the sarcomere (Ono, 2003) and before our work it was unclear if they could also be used to regulate membrane extension within muscle cells.

Here we present a detailed characterization of muscle arm development and have found it to be stereotypical, suggesting a high degree of genetic regulation. We also show that perturbation of various components of the actin and myosin machinery, including actin, tropomyosin, ADF/cofilin and muscle myosin, impair muscle arm extension and disrupt arm

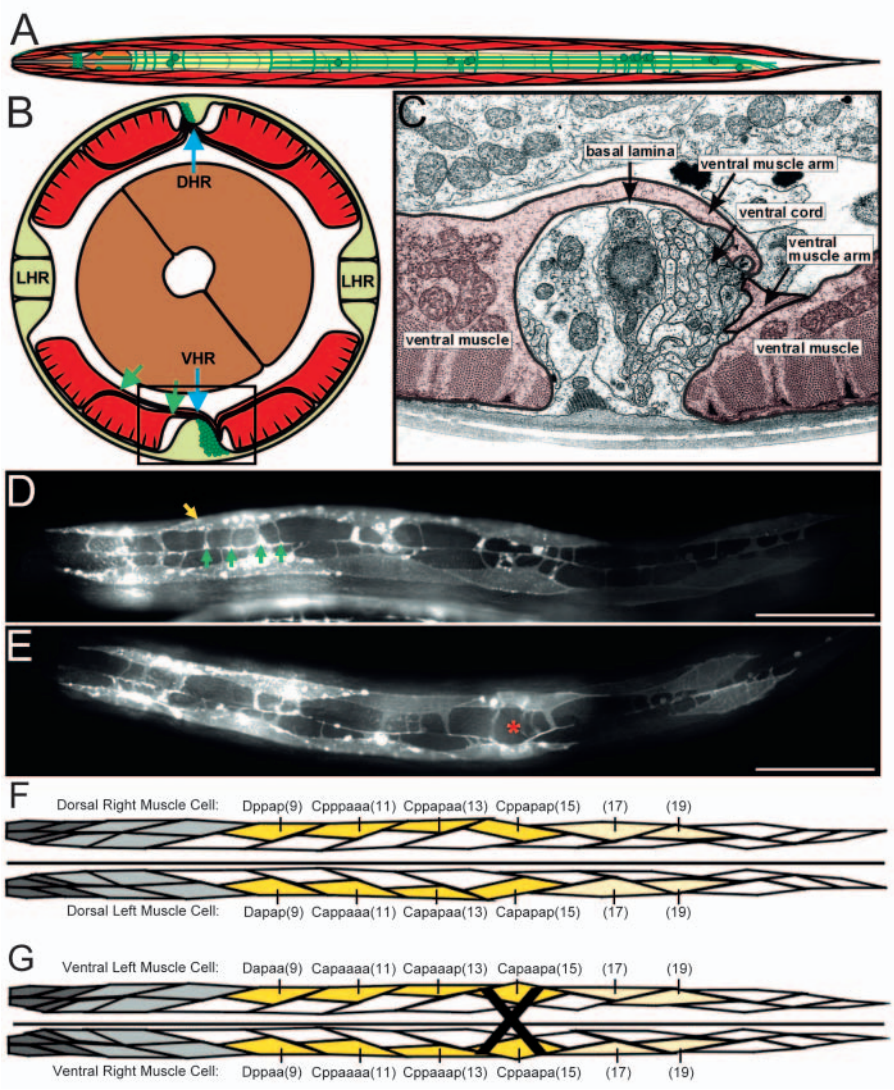

Fig. 1. The muscle arms of *C. elegans*. (A) An illustration of the BWMs (red) of the left side of *C. elegans*. Each BWM quadrant is organized into two rows. (B) A cross-section of A adapted, with permission, from White et al. (White et al., 1986). Each muscle of the two dorsal BWM quadrants and each muscle of the two ventral quadrants (red) extends arms to the nearest nerve cord (dark green) in either the DHR or the VHR, respectively. Only the muscle arms of the ventral left quadrant are indicated by green arrows. The LHR is indicated. (C) A transmission electron micrograph by John White (with permission) of the boxed region in B. BWMs are shaded pink. (D) The dorsal right (top) and dorsal left (bottom) BWMs that express MB::YFP from the *trIs30* integrated transgene in a young adult. The Cpppaaa BWM is indicated (yellow arrow), along with four muscle arms (green arrows). (E) The ventral left (top) and ventral right (bottom) BWMs. The red asterisk indicates the position of the vulva. (F,G) Tracings of the dorsal and ventral BWMs, respectively. The identities of the distal muscles that express Mb::YFP at high levels are bright yellow, and those that express Mb::YFP at lower levels are light yellow. The head BWMs are shaded in dark grey, while the neck BWMs are shaded in light grey. The black 'X' in (G) represents the vulval muscles, which do not express Mb::YFP from *trIs30* transgene. Anterior is to the left in all panels except in B and C. Scale bars: 50 μm. DHR, dorsal hypodermal ridge; LHR, lateral hypodermal ridge; VHR, ventral hypodermal ridge.

morphology. Our work has resulted in new insights about the mechanics of membrane extension in muscle cells and establishes *C. elegans* muscle arms as a useful in vivo model for membrane extension.

Materials and methods

Nematode strains and transgenics

Unless otherwise indicated, nematodes were cultured at 20°C. RP247 *trIs30 I* was constructed by microinjecting *pPRRF138.2(him-4p::MB::YFP)*, *pPRZL44(hmr-1b::DsRed2)* and *pPR2.1(unc-129neural-specific promoter::DsRed2)* together at 10, 80 and 40 ng/μl, respectively, into N2 (wild-type) adults using standard techniques (Mello et al., 1991). The membrane anchor sequence (Mb) used to localize YFP was obtained from Dr A. Fire's 1999 vector kit and is from the *pat-3* membrane-localization domain (Gettner et al., 1995). An extra-chromosomal array of *trEx[pPRRF138.2; pPRZL44; pPR2.1]* was integrated using a previously described protocol (Mitani, 1995). Resulting integrants were backcrossed to N2 four times. RP127 *trIs25* was constructed similarly by injecting and integrating *pPRRF138.2(him-4p::MB::YFP)*, *pPRZL47(F25B3.3p::DsRed2)* and *pRF4(rol-6(su1006)* into N2, at 20, 50 and 50 ng/μl, respectively. The pPRRF207*(him-4p::gfp::act-1)* transgene was generated by ligating a 5.6 kb *Eco*RI-*Asp*718 fragment from *pPRZL138.1(him-4p::YFP)* to the 2.4 kb *Asp*718-*Eco*RI fragment from *pJH4.64(pei-1p::GFP::act-1)*, which was a generous gift from Geraldine Seydoux. We used this transgene instead of a phalloidin conjugate that binds to all actin because the actin within BWMs obscures visualization of the actin within the relatively long distal BWM arms (not shown).

To investigate larval muscle arm extension in a post-embryonic cell division mutant we made *lin-6(e1466) dpy-5(e61)/hT2[qIs48]* (Wang and Kimble, 2001) animals transgenic for *him-4p::Mb::YFP*. *lin-6(e1466)* homozygotes are easily recognized, as the mutation is linked to *dpy-5(e61),* which has a distinct phenotype. Post-embryonic divisions occur in *lin-6(e1466)* mutants, but most daughter cells eventually die (Sulston and Horvitz, 1981). The molecular identity of *lin-6* is not published.

Microscopy, temperature shift experiments and statistical analysis

For microscopy, worms were anaesthetized in 2-10 mmol/l Levamisole (Sigma) in M9 solution (Lewis, 1995) and mounted on a 2% agarose pad. We used a Leica DMRA2 HC microscope with standard Leica filter sets for GFP, YFP, CGFP and GFP Red epi-fluorescence to take all pictures. A 20× dry objective was used to take all pictures of adult worms, while a 63× oil objective was used to take pictures of young larvae and GFP::actin-expressing muscles. All muscle arm counts were done from photographs, which are available upon request. To study populations of worms at defined developmental stages, worms were first synchronized (Lewis, 1995) and then staged by the extent of germline and gonad cell proliferation (Kimble and Hirsh, 1979).

The temperature-shift experiments were done by incubating worms at either 15 or 25°C for at least 24 hours. Synchronized L1s (Lewis, 1995) were deposited on plates with food and placed at the desired temperature. The developmental stage of the worms was monitored and pictures of the dorsal right muscle quadrants were taken when the animals reached adulthood.

We did not assume Gaussian distributions of the number of counted arms and therefore used a more

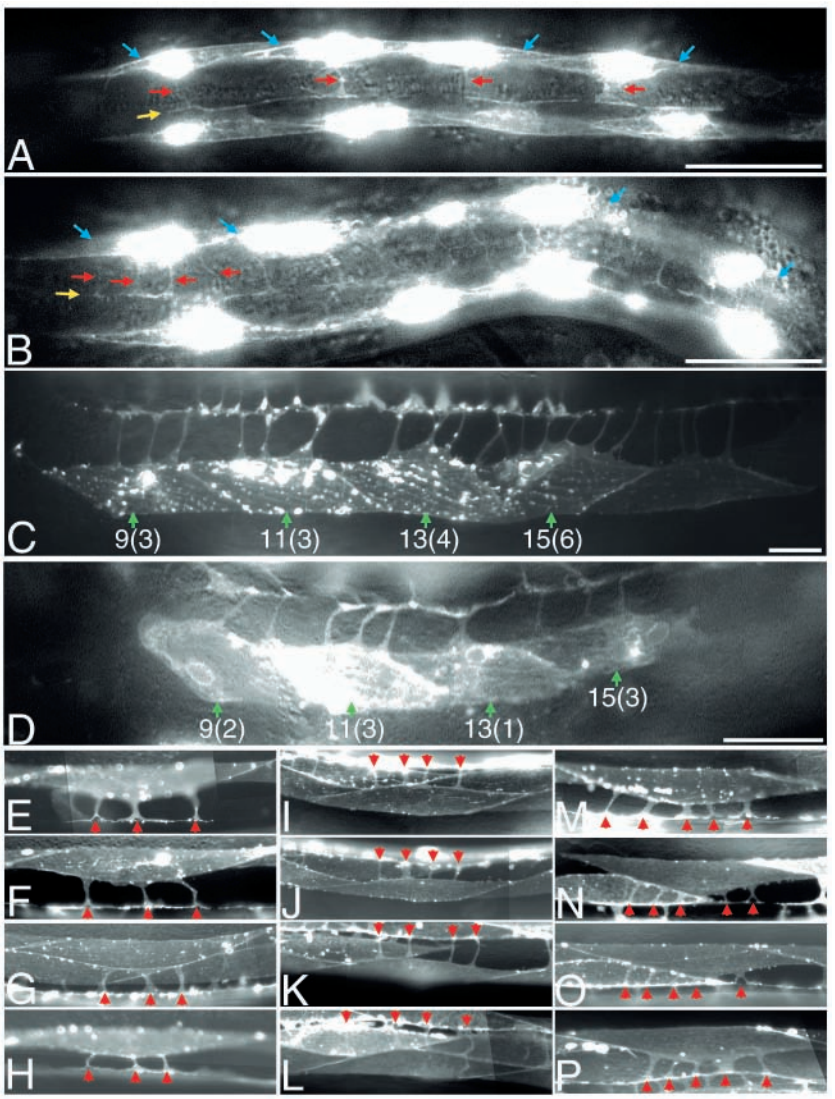

Fig. 2. Larval muscle arm outgrowth and migration. (A) Dorsal view of eight BWMs of an early RP127 *trIs25* L1. Muscles 9-15 of the dorsal right quadrant (blue arrows) each BWM extends a single arm (red arrow) to the dorsal cord (yellow arrow). (B) Dorsal view of the same eight BWMs as in A, but in a different animal of the early L2 stage. The four muscles of the dorsal right quadrant (blue arrows) extend 3-4 arms to the dorsal cord. In both A and B, anterior is to the left. (C) Four dorsal left BWMs of an adult RP242 *Ex[him-4p::MB::YFP; hmr-1b:: DsRed2; unc-129nsp:: DsRed2]; dpy-5(e61)* animal, which serves as the control for muscle arm counts in a *lin-6* mutant background. BWM identity numbers are shown, along with the number of muscle arms in brackets. (D) The same four BWMs as in C, but in an RP226 *Ex[him-4p::MB::YFP; hmr-1b:: DsRed2; unc-129nsp:: DsRed2]; lin-6(e1466) dpy-5(e61)* animal. (E-P) RP235 animals mosaic for *[myo-3p::Mb::YFP; unc-25p::DsRed; unc-129nsp::CFP]*. Muscle arms are indicated with a red arrowhead. (E-H) The same ventral left muscle 13 from four different animals. (I-L) The same dorsal right muscle 13 from four different animals. (M-P) The same ventral right muscle 13 from four different animals. Scale bars: 20 μm.

Table 1. The number of muscle arms at various developmental time points and in animals lacking post-embryonic motoneurons

Genotype	*n*	Quadrant*	9†	11†	13†	15†	17†b	19†	Average
trIs30 (early L1s)	30	Vr	1.3±0.5	1.5±0.6	2.0±0.7	1.7±0.7	–	–	1.6
trIs30 (early L1s)	30	Vl	1.5±0.7	1.3±0.5	1.4±0.5	2.0±0.6	–	–	1.5
trIs30 (early L1s)	30	Dr	1.3±0.5	2.1±1.1	1.6±0.6	1.7±0.7	–	–	1.7
trIs30 (early L1s)	30	Dl	1.3±0.5	1.8±0.7	1.9±0.8	2.7±1.2	–	–	1.9
trIs30 (late L2s)	30	Vr	3.4±0.8	3.5±0.9	3.7±0.8	3.8±1.5	–	–	3.6
trIs30 (late L2s)	30	Vl	3.4±0.7	3.3±1.1	3.2±0.9	4.0±1.2	–	–	3.4
trIs30 (late L2s)	30	Dr	2.8±0.8	3.0±0.8	2.7±0.8	3.2±0.9	–	–	2.9
trIs30 (late L2s)	30	Dl	3.5±0.8	3.8±1.0	3.2±0.9	4.4±0.9	–	–	3.7
trIs30 (young adults)	30	Vr	4.1±0.9	4.6±1.0	4.7±0.8	4.8±1.0	3.4±0.8	5.8±1.2	4.6 (4.5)
trIs30 (young adults)	30	Vl	3.6±0.8	3.4±0.8	3.6±0.8	3.7±0.9	2.4±1.0	4.5±1.1	3.5 (3.6)
trIs30 (young adults)	30	Dr	3.2±0.9	3.5±0.7	3.6±0.8	4.0±0.9	2.8±0.7	4.1±0.7	3.5 (3.6)
trIs30 (young adults)	30	Dl	3.7±0.8	3.8±0.9	4.2±1.1	4.8±0.9	2.7±0.7	3.6±1.0	3.8 (4.1)
Ex[him-4p::Mb::YFP]; lin-6(e1466) dpy-5(e61)	10	Vr	1.7±0.7	1.8±0.8	2.1±0.3	2.0±0.5	–	–	1.9
Ex[him-4p::Mb::YFP]; lin-6(e1466) dpy-5(e61)	10	Vl	2.1±0.6	2.1±0.7	1.9±0.7	2.3±0.5	–	–	2.1
Ex[him-4p::Mb::YFP]; lin-6(e1466) dpy-5(e61)	10	Dr	2.5±0.9	2.3±0.5	2.6±1.0	2.7±0.8	–	–	2.5
Ex[him-4p::Mb::YFP]; lin-6(e1466) dpy-5(e61)	10	Dl	2.8±0.8	2.6±1.0	2.3±1.3	2.9±1.0	–	–	2.7
Ex[him-4p::Mb::YFP]; dpy-5(e61)	15	Vr	3.7±0.7	3.7±0.6	3.7±0.9	3.9±0.7	–	–	3.8
Ex[him-4p::Mb::YFP]; dpy-5(e61)	15	Vl	3.5±0.6	3.4±0.5	3.6±0.5	3.6±0.5	–	–	3.5
Ex[him-4p::Mb::YFP]; dpy-5(e61)	15	Dr	3.4±0.5	3.5±0.8	3.3±0.6	3.9±0.5	–	–	3.6
Ex[him-4p::Mb::YFP]; dpy-5(e61)	15	Dl	3.5±0.8	3.7±0.8	3.5±0.5	4.3±1.2	–	–	3.8

*The BWM quadrants are as follows: Vr, ventral right; Vl, ventral left; Dr, dorsal right; Dl, dorsal left.
†Shown are the average numbers of muscle arms for each of the indicated muscles, followed by the s.d.
‡The average number of muscle arms for all muscles considered within the indicated quadrant. The numbers in brackets in the last column are the averages for muscles 9, 11, 13 and 15.

stringent two-tailed Mann-Whitney rank sum test to assess the statistical significance of the observed differences.

RNAi

All RNAi experiments were done by feeding worms dsRNA-producing bacteria as previously described (Timmons and Fire, 1998). The *pPRRF215 unc-54(RNAi)* construct was made by isolating a 1700 bp *Pst*I-*Bgl*II *unc-54* genomic fragment that contains exons 4, 5 and the first 286 bp of exon 6 from the *pPD5.41 unc-54* genomic clone (a gift from Dr A. Fire) and sub-cloning it into the RNAi feeding vector pPD129.36 (Timmons and Fire, 1998) cut with *Pst*I and *Bgl*II. *pPRRF215* and the negative control (empty pPD129.36) vector were transformed into HT115 bacteria (Timmons et al., 2001) using standard protocols.

Muscle arm width analysis

The width of muscle arms from dorsal right BWM number 11 was measured for ten young adult animals of each genotype using Openlab 3.1.5 software (Improvision Inc.). Arm width was measured at the midpoint of each arm, halfway between the body of the muscle and the nerve cord. Because the length of worms, and therefore the length or size of BWMs, can vary substantially between adults of different ages and of different genetic backgrounds, the arm widths were normalized to the total muscle length along the anterior-posterior axis to control for differences in animal size.

Results

Muscle arms can be visualized using membrane-anchored yellow-fluorescent protein

To better understand muscle arm biology in *C. elegans*, we performed a detailed analysis of muscle arm development. We examined muscle arms in populations of live hermaphrodite animals expressing membrane-anchored yellow-fluorescent protein (Mb::YFP) from the muscle-specific *him-4* promoter (*him-4p*) (Vogel and Hedgecock, 2001) (Fig. 1). This marker was used because it is expressed in only a subset of distal BWMs and therefore enables the clear visualization of individual muscle arms.

Expression of Mb::YFP from *him-4p* in first larval-stage (L1) larvae was limited to four distal BMWs posterior to the neck muscles in each quadrant (Fig. 2A). As development continued, two more distal BWMs posterior to the initial four in each quadrant also expressed Mb::YFP, albeit at lower levels (Fig. 1D,E). We were able to assign unambiguous identities to the 16 BWMs that expressed Mb::YFP brightly from *him-4p* because of the largely invariant cell lineage and the stereotypical pattern of BWM shapes and arrangements (Sulston and Horvitz, 1977; Sulston et al., 1983). For example, the dorsal right BWM Cppapap is the most anterior muscle that is always overlapped by neighbouring BWMs on either side and can therefore serve as a useful position marker (Fig. 1F). There are 14 BWMs born post-embryonically from the M-mesoblast cell that intercalate into the existing quadrants at variable positions (Sulston and Horvitz, 1977). The general integration space is posterior to the gonad primordium, which is located just posterior to the four brightly fluorescing BWMs. The identities we assigned to the posterior muscles that fluoresced lightly are therefore based on position only and not lineage. For convenience we have renamed the BWMs with numbers according to their position along the anterior-posterior axis in each quadrant. For example, Cppapap is referred to as dorsal right muscle 15 (Fig. 1F,G).

To control for the possibility that the Mb::YFP muscle arm reporter may interfere with muscle arm outgrowth, migration or morphology, we examined BWMs expressing DsRed2 driven from the muscle-specific *C26G2.1* promoter (P.J.R. and S. Quaggin, unpublished). There were no differences in arm morphology or the number of arms observed with the two different reporters (not shown and Table 2, line 35). We

Table 2. A comparison of the number of muscle arms in various mutant backgrounds from body wall muscles of the dorsal right quadrant

	Genotype*	Description	Mean†	P‡	P§
1	*trIs30* (15°C)	Wild-type young adults	3.8±1.1	ns	–
2	*trIs30* (20°C)	Wild-type young adults	3.5±0.9	–	–
3	*trIs30* (25°C)	Wild-type young adults	3.7±1.0	ns	–
4	*trIs30(0RNAi)*	Wild-type young adults	3.5±0.8	ns	–
5	*trIs30* (20°C)	Wild-type L1 hatchlings	1.7±0.8¶	<0.001	–
6	*sma-6(e1482)*	Tgf-β receptor (small worms)	3.4±0.8	ns	–
7	*lon-2(e678)*	Glypican (long worms)	3.7±1.2	ns	–
8	*dpy-5(e61)*¶	Collagen (short worms)	3.6±0.7¶	ns	–
9	*dyp-10(e128)*	Collagen (control for *unc-104* null)	3.6±0.9¶	ns	–
10	*act-1,2,3(st15)*	Actin	2.4±1.0¶	<0.001	<0.001 (5)
11	*unc-60(su158)*	ADF/cofilin (null)	1.8±0.9	<0.001	ns (5)
12	*unc-60(e723)*	ADF/cofilin (hypomorph)	1.8±0.8	<0.001	ns (5)
13	*unc-60(s1307)*	ADF/cofilin (hypermorph)	3.3±1.0	ns	<0.001 (11)
14	*unc-60(r398)*	ADF/cofilin (no severing)	3.3±1.2	ns	<0.001 (11)
15	*unc-78(gk27)*	Actin-interacting protein 1 (null)	3.4±1.0	ns	–
16	*lev-11(TM1-RNAi)*	Tropomyosin	2.1±1.0	<0.001	ns (5)
17	*lev-11(TM2-RNAi)*	Tropomyosin	2.2±1.1	<0.001	0.038 (5)
18	*act-1,2,3(st15); lev-11(TM1-RNAi)*	–	1.7±0.8¶	<0.001	ns (15)/ns (5)
19	*unc-60(su158); lev-11(TM1-RNAi)*	–	1.4±0.6¶	<0.001	ns (10)/ns (5)
20	*unc-54(e190)*	Muscle myosin (MHC B) (null)	2.4±1.1	<0.001	<0.001 (5)
21	*unc-54(e190)*	*unc-54* L1 hatchlings (null)	1.7±0.7¶	<0.001	ns (5)
22	*unc-54(e1152)*	Muscle myosin (MHC B)	2.3±1.1	<0.001	–
23	*unc-54(RNAi)*	Muscle myosin (MHC B)	2.3±1.2	<0.001	ns (20)
24	*unc-15(e73)*¶	Paramyosin	2.7±1.1	<0.001	–
25	*unc-15(su2000)*¶	Paramyosin	3.0±1.0	<0.001	–
26	*unc-15(RNAi)*	Paramyosin	3.1±1.2	<0.001	0.007 (24)
27	*unc-15(e1402ts)* (25°C)¶	Paramyosin	3.1±1.0	0.003	–
28	*unc-54(e190); lev-11(TM1-RNAi)*	–	2.1±0.9	<0.001	–
29	*act-1,2,3(st15); unc-54(RNAi)*	–	2.9±0.9¶	<0.001	0.037 (10)
30	*unc-60(su158); unc-54(RNAi)*	–	1.6±0.8	<0.001	ns (11)
31	*unc-104(e1265)*	Kinesin	1.7±1.2	<0.001	ns (5)
32	*unc-104(rh43)*	Kinesin	1.3±1.0	<0.001	0.011 (5)
33	*unc-104(rh142) dyp-10(e128)*	*unc-104* null	1.2±0.6¶	<0.001	<0.001 (5)
34	*egl-30(n715)*	G protein α-subunit	3.7±1.0	ns	–
35	*C26G2.1p::DsRed2*	Control for Mb::YFP	3.8±0.7	ns	–

*All counts were made in the *trIs30* background, except ¶, which were carried out with a *him-4p::Mb::YFP* extra-chromosomal array. All counts are from young adults raised at 20°C unless otherwise indicated.

†Shown is the average number of muscle arms per BWM for the dorsal right quadrant, followed by the s.d. Only BWMs 9, 11, 13, 15, 17 and 19 were considered, except ¶, where BWMs 9, 11, 13 and 15 were considered. The arms of 15 muscles of each type were counted for each genotype, except for *trIs30* at 20°C and *trIs30* hatchlings, where 30 muscles of each type were counted.

‡These P values were derived from Mann-Whitney tests with respect to the *trIs30* counts (row 2).

§These P values were derived from Mann-Whitney tests with respect to the counts from the row indicated in brackets. ns, not significant (P>0.05). For those counts where only muscles 9-15 were considered, all statistical tests were carried out by comparing these counts to that of muscles 9-15 of the respective genotypes. The mean number of arms for each muscle is shown in Table S1 in the supplementary material.

conclude that Mb::YFP driven from *him-4p* does not interfere with muscle arm number or morphology and is therefore a useful tool to study muscle membrane extension.

Muscle arm extension is a highly regulated and stereotypical process

Previous work has shown that L1 larvae have one or two muscle arms per BWM, whereas adults have three to five muscle arms per BWM (Hall and Hedgecock, 1991; Hedgecock et al., 1990). The period of muscle arm extension and migration during larval development was not known at the initiation of our studies. To determine when larval muscle arm extension occurs we therefore counted muscle arms at three developmental stages (Table 1). Newly hatched animals had on average 1.7 (±0.8; n=480) muscle arms per BWM (Fig. 2A). We infer that these arms develop during embryogenesis as previously suggested (Hedgecock et al., 1990). By the second larval stage, distal BWMs extended an average of 3.4 (±1.0; n=320) muscle arms (Fig. 2B). This indicates that there is a burst of muscle arm extension after hatching and before the completion of L2 development. The number of muscle arms in adults (μ=4.0±1.0; n=480) suggests that additional arm extension occurs after the second larval stage (P<0.001).

The major period of larval muscle arm outgrowth is coincidental with the only period of post-embryonic motoneuron proliferation in hermaphrodites (Sulston and Horvitz, 1977). This coincidence raised the possibility that post-embryonic motoneurons induce larval muscle arm outgrowth. We reasoned that if larval muscle arm outgrowth is dependant on the birth of post-embryonic motoneurons, *lin-6* mutant animals, which are defective for post-embryonic DNA replication (Sulston and Horvitz, 1981), should have fewer muscle arms than controls. *lin-6(e1466) dpy-5(e61)* adults had an average of 2.3 (±0.8; n=160) muscle arms per BWM, which is significantly less than wild type (μ=4.0±1.0; n=480) and *dpy-5(e61)* controls (μ=3.6±0.7; n=235) (P<0.001) (Fig. 2,

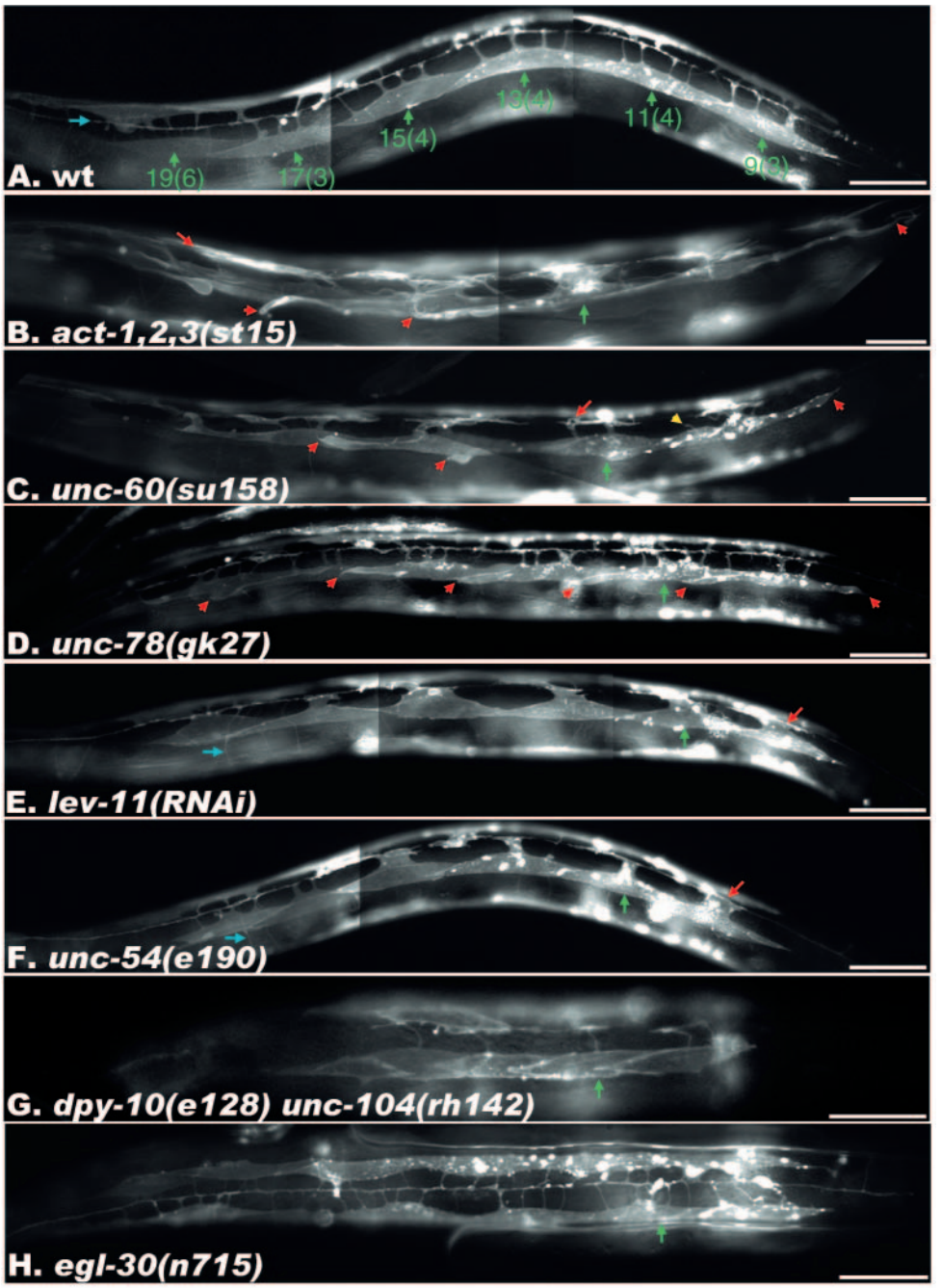

Fig. 3. Mutant muscle arm phenotypes. In all panels, BWMs of the dorsal right quadrant are shown. Dorsal is up, and anterior is to the right. All animals shown contain the *trIs30* transgene. (A) An RP247 *trIs30* animal with muscles 9-19 indicated with the number of muscle arms shown in brackets. The dorsal cord (not shown) is indicated with the blue arrow. In all subsequent panels, muscle number 11 is indicated with a green arrow for reference, select muscle arm termini defects are indicated with a red arrow, some flowing lateral muscle ends are indicated with a red arrowhead. (B) Note the arborized muscle arms (red arrow) and flowing lateral muscle ends (red arrowheads). (C) Note the fewer muscle arms, the errant membrane projections (yellow arrowhead), and flowing lateral muscle ends (red arrowhead). A commissural neuron whose fluorescence is bleeding through to the YFP channel is indicated with a blue arrow in E-H. Scale bars: 50 μm.

Table 1). These results are consistent with the hypothesis that muscle arm outgrowth during larval development requires post-embryonic motoneuron proliferation.

We next examined the number of muscle arms extended by BWMs 9 to 19 in each quadrant in detail. The number of arms extended by different BWMs within the same quadrant was significantly different (P<0.001) (Table 1). In the ventral left quadrant, for example, muscle 11 extended an average of 4.6 arms, muscle 17 extended an average of 3.4 arms, and muscle 19 extended an average of 5.8 arms. A visual inspection of the position of muscle arm outgrowth from BWMs, the paths taken to the nerve cord, and the morphology of the arms suggest that muscle arm outgrowth and migration is also stereotypical (Fig. 2E-P). These results suggest the existence of extensive genetic regulation that controls several aspects of muscle arm development.

The UNC-104 kinesin motor protein is thought to transport the putative muscle arm chemoattractant along motor axons (Hall and Hedgecock, 1991). We therefore counted the number of muscle arms extended in the background of three *unc-104* loss-of-function mutations, including the null mutation *rh142* (Hall and Hedgecock, 1991). In this and all further mutant analysis we considered the muscle arms only from the dorsal right quadrant BWMs, as all quadrants show similar defects and muscle arms are most clearly visible in this quadrant. The *unc-104* mutants displayed significantly fewer muscle arms than did wild-type adult animals (P<0.001) (Table 2, lines 31-33; Fig. 3). Intriguingly, *unc-104* mutant adults extended

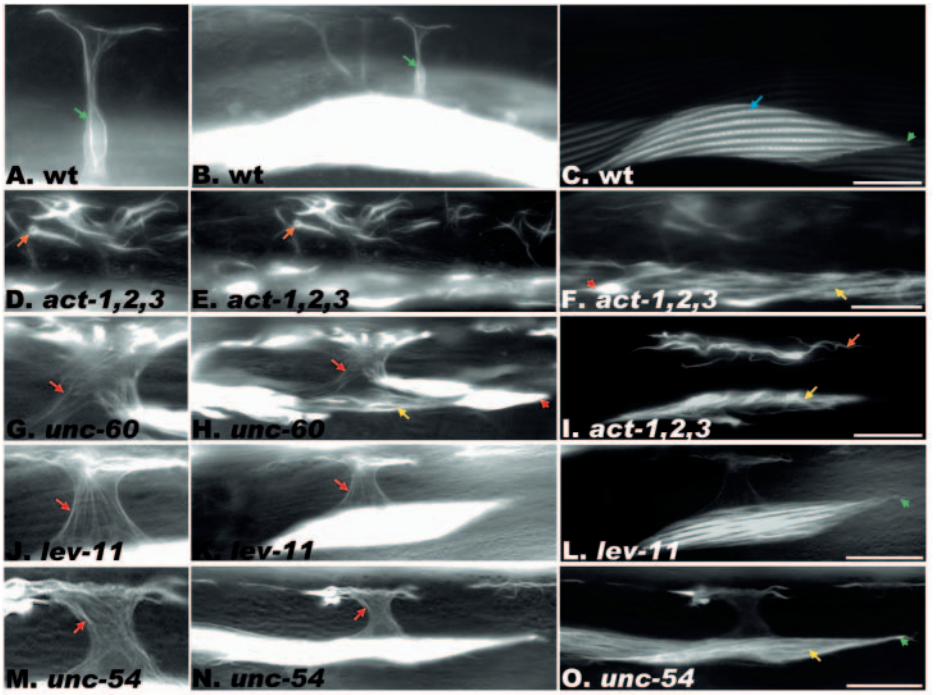

Fig. 4. Actin distribution in muscle arms. All muscles shown express GFP::ACT-1 from the extra-chromosomal array *trEx[pPRRF207(him-4p::gfp::act-1)* in the background of the *dpy-5(e61)* mutation, which enables better visualization of the muscle arms. (A-C) GFP::ACT-1 in a wild-type background. (A) Magnification of the muscle arm shown in B. Note the long actin cables in A and B (green arrows). (C) A lighter exposure of the same muscle depicted in B. Note the incorporation of GFP::ACT-1 in the thin filaments (blue arrow). Orange arrows point to arborized arm termini, yellow arrows point to disorganized sarcomeres, red arrows point to actin bundles within arms, green arrowheads point to discrete muscle lateral ends, and red arrowheads point to enriched actin in flowing lateral ends of muscle. Scale bars: 25 μm.

similar numbers of muscle arms to wild-type hatchlings. This suggests that UNC-104 is required for larval muscle arm outgrowth, but is dispensable for embryonic muscle arm development.

A dominant actin mutation disrupts muscle arm development

Membrane extension is dependent upon remodelling of the actin cytoskeleton (Pollard and Borisy, 2003; Ritzenthaler et al., 2000), prompting us to determine if the actin cytoskeleton is required for muscle arm extension. To visualize actin in muscle arms we used the *him-4* promoter to drive the expression of a GFP-*C. elegans* actin (ACT-1) fusion protein within the distal BWMs (Fig. 4). Similar functional GFP::ACTIN fusion proteins have been used in many other systems to investigate the subcellular distribution of actin (Fischer et al., 1998; Jacinto et al., 2002; Uchida and Yumura, 2004). In several lines made transgenic for *him-4p*::GFP::ACT-1 we observed GFP fluorescence in the isotropic bands of the BWM sarcomeres in a characteristic pattern that surrounds dense bodies (Fig. 4C) (Francis and Waterston, 1985). This demonstrates that the GFP::ACT-1 fusion protein is properly localized. In the muscle arms of these animals, actin bundles were typically observed along the shaft and occasionally at the branched termini (Fig. 4A).

Actin loss-of-function mutations have no obvious phenotype, probably because of genetic redundancy. We therefore used an actin gain-of-function mutation *(st15)* to examine the consequences of actin perturbation on muscle arm development. The *act-1,2,3(st15)* allele is a mutation within the actin gene cluster *act-1,2,3*, although it is unknown which of the three actin genes is mutated (Landel et al., 1984; Waterston et al., 1984). We observed three muscle arm phenotypes in the *act-1,2,3(st15)* background. First, *act-1,2,3(st15)* adults had significantly fewer arms than controls, but more than L1 hatchlings (Table 2, line 10). Second, 91% of the mutant BWMs extended membrane in the general direction of the nearest nerve cord but did not make contact with it, compared with 10% of controls (Fig. 3, Table 3). We refer to this phenotype as errant membrane projections. Third, there was a

Table 3. An analysis of BWM membrane extension defects in various genetic backgrounds

Genotype	% of muscles with flowing lateral ends	% of muscles with errant membrane projections	% of muscles with arborized arm termini
Wild type	0	3	0
0(RNAi)	0	10	2
act-1,2,3(st15); 0(RNAi)	73	91	63
unc-60(su158); 0(RNAi)	100	70	29
unc-78(gk27)	91	26	3
lev-11(RNAi)	0	10	6
unc-54(RNAi)	2	3	8
act-1,2,3(st15); lev-11(RNAi)	11	14	45
unc-60(su158); lev-11(RNAi)	83	19	17
act-1,2,3(st15); unc-54(RNAi)	29	43	97
unc-60(su158); unc-54(RNAi)	100	78	90

One-hundred dorsal right muscles [25 of each of muscles 9-15 (see Fig. 1)] were counted for each genotype. *trIs30* is in the background of all animals.

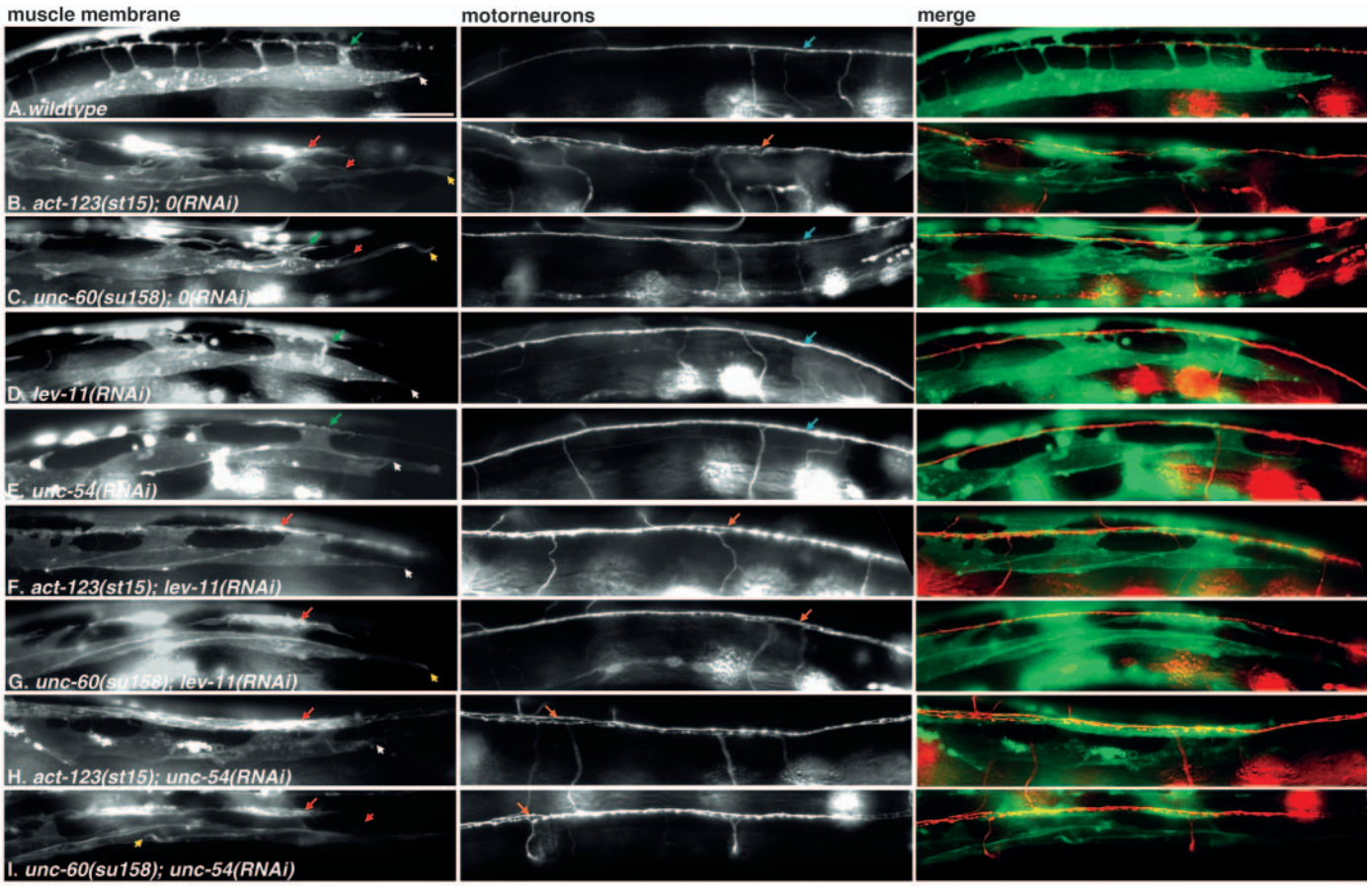

Fig. 5. *unc-54(RNAi)* interacts with *act-1,2,3(st15)* and *unc-60(su158)* to generate highly arborized muscle arm termini. All animals shown contain the *trIs30* transgene and express Mb::YFP in select BWMs, and DsRed2 in commissural motoneurons. Muscles 9 and 11 of the dorsal right quadrant are shown in the first column, the corresponding motoneurons in the middle column, and the merged image, with YFP false coloured green, is in the third column. Red arrows indicate arborized muscle arm termini, while green arrows indicate normal muscle arm termini, irrespective of the defects of the arm stalk. Red arrowheads indicate membrane extension defects, yellow arrowheads indicate errant flowing lateral muscle ends, while white arrowheads indicate discrete lateral muscle ends. In the second column, blue arrows indicate a normal dorsal cord, while an orange arrow indicates a defasciculated dorsal nerve cord. Note that the defasciculated nerve cords correlate with muscle arm termini arborization. Also note that in *unc-60(su158); lev-11(RNAi)* (G) and in *unc-60(su158); unc-54(RNAi)* (I) animals, the nerve cords are defasciculated, where none of the single mutants or RNAi-treatments result in defasciculated cords (C-E). Scale bars: 25 μm.

dramatic arborization of muscle arm termini at the nerve cords (Fig. 3, Table 3). In addition to these arm phenotypes, 73% of *act-1,2,3(st15)* BWMs had flowing lateral ends (Fig. 3B), which differed significantly in morphology from the pointed lateral ends of wild-type controls (Table 3). We also examined the distribution of actin in the *st15* mutant background using the GFP::ACT-1 reporter. We found that muscle arm termini in *act-1,2,3(st15)* mutants were enriched with actin compared with controls (Fig. 4). Moreover, we were unable to resolve individual actin filaments or actin filament bundles within the arm termini. These results demonstrate a crucial role for actin regulation in muscle arm development.

UNC-60B/ADF/cofilin is required for muscle arm extension

We investigated the consequences of disrupting actin dynamics on muscle arm extension. We first examined the role of ADF/cofilin, which has both actin-severing and actin depolymerization activities and is required for membrane extension in many cell types (Maciver and Hussey, 2002). The *C. elegans* genome encodes a single ADF/cofilin gene, *unc-60*. The *unc-60* mRNA is spliced in two ways from a common first exon encoding only the initiator methionine to give two distinct ADF/cofilin orthologues: UNC-60A and UNC-60B (McKim et al., 1994). While UNC-60A is widely expressed, UNC-60B is specifically expressed in BWMs, vulva and spermatheca (Ono et al., 2003). Although deletions of *unc-60A* are lethal, all alleles of *unc-60B* are viable and result in defective BWM sarcomeres (Ono et al., 2003; Ono et al., 1999).

We observed three muscle arm phenotypes in *unc-60B(su158)* animals. First, *unc-60B(su158)* animals have as few muscle arms as wild-type L1 hatchlings (Fig. 3) (Table 2, line 11). This suggests that larval muscle arm extension is abrogated in animals lacking UNC-60B. Second, 70% of *unc-60B(su158)* BWMs have errant membrane projections (Fig. 3) (Table 3). Third, 29% of *unc-60B(su158)* BWMs have arborized arm termini, compared to 2% of controls (Table 3). In addition, 100% of the BWMs in an *unc-60B(su158)* background have flowing lateral ends, compared to none in controls (Fig. 3) (Table 3). The F-actin bundles in the muscle

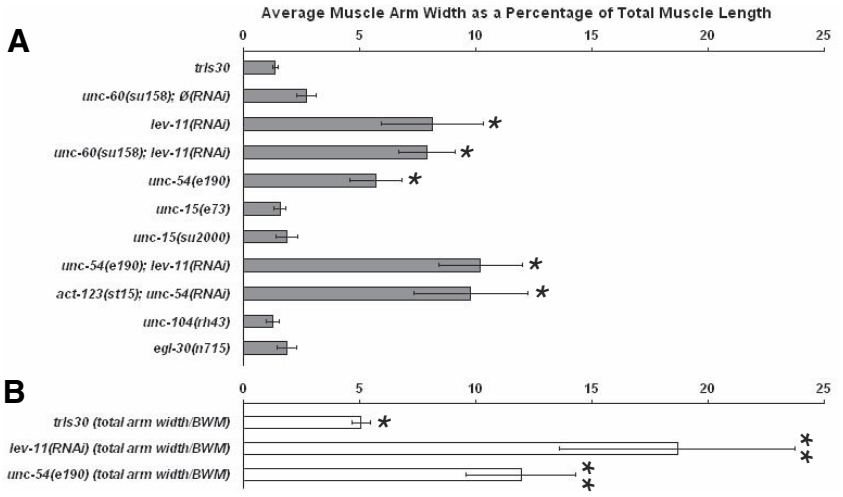

Fig. 6. A comparison of average muscle arm widths. (A) The muscle arm widths are expressed as an average percentage of muscle cell length (see Materials and methods). (B) The average total arm width per BWM for select genotypes. A single asterisk at the end of the bars indicates a significant difference with *trIs30* ($P<0.001$) (grey bar). A double asterisk at the end of the bars indicates a significant difference with the total arm width of *trIs30* controls (white bar) ($P<0.001$). All animals were raised at 20°C. Errors bars represent the standard error of the mean.

arms of *unc-60B(su158)* mutants appear disorganized in the shaft and there is an accumulation of actin fibres within the muscle arm termini, similar to *act-1,2,3(st15)* mutants (Fig. 4). These results suggest an important role for UNC-60B-mediated actin regulation in muscle arm extension.

Wild-type UNC-60B can both depolymerize and sever F-actin. The *unc-60B(e723)* mutation, however, severely reduces both these activities, while *s1307* enhances both activities, and *r398* enhances depolymerization but eliminates severing (Ono et al., 1999). To investigate which activities are required for muscle arm extension, we examined muscle arms in these three *unc-60B* mutants (Table 2, lines 12-14). As expected, *e723* adults had similar numbers of muscle arms to *unc-60B(su158)* null mutants and wild-type hatchlings ($P>0.05$). Conversely, *unc-60B(s1307)* mutants had similar numbers of muscle arms to wild-type adults ($P>0.05$). Interestingly, *unc-60B(r398)* mutants also had wild-type numbers of muscle arms ($P>0.05$). Because *r398* retains F-actin depolymerization activity but has no severing activity, we conclude that UNC-60B-mediated severing is dispensable for muscle arm extension. One interpretation of this result is that the depolymerization activity of UNC-60B ensures that a pool of free G-actin is available for new arm extension.

Actin filament disassembly by UNC-60B is strongly enhanced by UNC-78, an actin–interacting protein 1 (AIP1) orthologue expressed in BWMs (Mohri and Ono, 2003; Ono et al., 2004). We therefore hypothesized that *unc-78* mutants might also have muscle arm extension defects. Although the BWMs of *unc-78(gk27)* null mutants exhibit a similar number of lateral flowing ends to *unc-60B(su158)* (Fig. 3, Table 3), the number of muscle arms extended in *unc-78(gk27)* mutants did not differ significantly from controls (Table 2, line 15). This result suggests that the muscle arm defects observed in *unc-60B(su158)* and *unc-60B(e723)* mutants are not a secondary consequence of defects within the sarcomere, because sarcomere organization is similarly disrupted in *unc-60B* and *unc-78* nulls (Ono et al., 2001).

Tropomyosin is required for both muscle arm extension and morphology

ADF/cofilin-dependent actin disassembly is antagonized by tropomyosin, which structurally reinforces actin filaments (Bernstein and Bamburg, 1982; Blanchoin et al., 2000; DesMarais et al., 2002; Ono and Ono, 2002). We investigated whether *C. elegans* tropomyosin, called LEV-11 or TMY-1, might also be required for muscle arm extension. We examined muscle arms in two different *lev-11(RNAi)* backgrounds. *lev-11(TM1-RNAi)* targets the two *lev-11* isoforms that are thought to be muscle-specific, while *lev-11(TM2-RNAi)* targets isoforms that are expressed in BWMs, the pharynx and the intestine (Kagawa et al., 1995; Ono and Ono, 2002). Both *lev-11(TM1-RNAi)* and *lev-11(TM2-RNAi)* resulted in a significant reduction in the number of muscle arms in adults (Table 2, lines 16 and 17). We therefore restricted further *lev-11(RNAi)* analysis to the TM1 isoforms. As the number of muscle arms in *lev-11(RNAi)*-treated animals is wild-type hatchlings ($P>0.05$), we conclude that tropomyosin is essential for larval arm extension.

Tropomyosin stabilizes actin filaments (DesMarais et al., 2002; Ono and Ono, 2002). We therefore tested whether *lev-11(RNAi)* could suppress the membrane extension defects observed in *unc-60(su158)* and *act-1,2,3(st15)* mutants, which

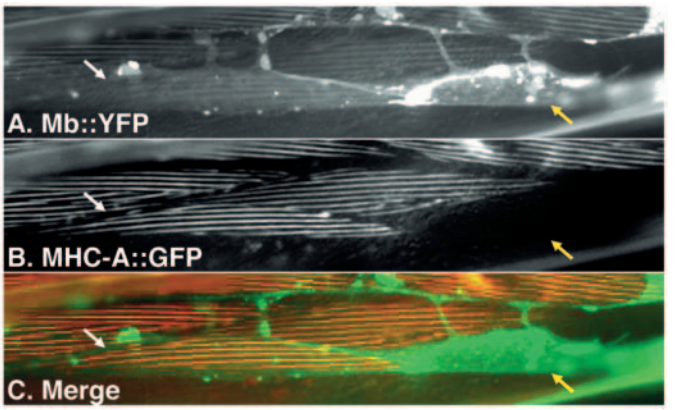

Fig. 7. Muscles mosaic for MHC-A::GFP. (A-C) The same muscles of the same RP339 *trIs30; myo-3(st386); stEx30[myo-3p::myo-3::gfp; pRF4(rol-6(su1006))]* animal (A) Muscles photographed with a YFP filter. Two muscles are indicated (white and yellow arrow) and both express Mb::YFP. (B) The same muscles in A photographed with a CFP filter to exclude the YFP signal, but to capture the GFP signal. One muscle expresses MHC-A::GFP (white arrow), while the other does not (yellow arrow). (C). Merge of A and B. YFP is false coloured green, and the GFP is false coloured red.

probably result from excessive actin filament extension or stability. We observed that *unc-60(su158); lev-11(RNAi)* worms had fewer BWMs with errant membrane projections (19% vs 70%), flowing lateral muscle ends (83% vs 100%), and fewer muscle arms with arborized arm termini (17% vs 29%) than *unc-60(su158)* mutants alone (Table 3). *lev-11(RNAi)* similarly reduced the membrane-associated defects observed in an *act-1,2,3(st15)* background (Table 3). These results show that *unc-60* and *lev-11* act antagonistically in BWMs and are consistent with previous in vitro studies (Ono and Ono, 2002).

Intriguingly, the muscle arms of *lev-11(RNAi)*-treated animals were dramatically wider than wild-type controls (Figs 3-6). These wide arms are unlikely to be an amalgamation of wild-type muscle arms, as the combined width of the remaining arms in *lev-11(RNAi)*-treated animals greatly exceeds the combined width of arms in wild-type worms (Fig. 6B). A model explaining the wide arms of *lev-11(RNAi)*-treated animals is presented in the discussion. In summary, these data indicate that *lev-11* is required for both larval muscle arm outgrowth and proper muscle arm morphology.

Muscle myosin is required for muscle arm extension and morphology

Many of the mutants and RNAi-treated animals that we have examined are not only predicted to have disrupted actin dynamics, but are also severely uncoordinated. To test if muscle arm development is dependent on locomotion, we examined muscle arms in the background of two mutations that result in severely uncoordinated movement but were not known to disrupt actin regulation. First, we examined muscle arms in animals mutant for *egl-30*, which encodes an α-subunit of heterotrimeric G protein (Brundage et al., 1996). *egl-30(n715)* mutants were paralyzed, but had no muscle arm phenotypes, demonstrating that paralysis alone does not disrupt muscle arm development (Table 2, line 34; Fig. 6). We then examined *unc-54*, which encodes muscle myosin heavy chain B (MHC-B) (MacLeod et al., 1977). Surprisingly, *unc-54* loss of function resulted in significantly fewer arms and greater arm widths than wild-type controls (Table 2, line 20; Fig. 6).

MHC-B is expressed in all muscles in *C. elegans* except for the pharynx (Ardizzi and Epstein, 1987; Okkema et al., 1993) and is one of three components of thick filaments in BWMs, together with MHC-A, encoded by *myo-3*, and paramyosin, which is encoded by *unc-15* (Kagawa et al., 1989; Miller et al., 1986; Schachat et al., 1977; Waterston et al., 1977). Because MHC-B is an integral component of thick filaments, we investigated if disruption of this structure is likely to be the primary cause of the muscle arm defects observed in *unc-54* nulls. First, we examined muscle arms in *unc-15* mutants, which contain MHC-B aggregates in the BWMs and do not form thick filaments (Waterston et al., 1977). Table 2 and Fig. 6 show that *unc-15* loss-of-function mutants exhibited only a small decrease in the number of muscle arms and no increase in muscle arm width. This suggests that wild-type thick filaments are dispensable for muscle arm development. Next, we examined muscle arms in reduction-of-function backgrounds of *myo-3*. As the two available *myo-3* mutants are lethal, we first examined *myo-3* reduction-of-function by RNAi and found no muscle arm defects in either a wild-type

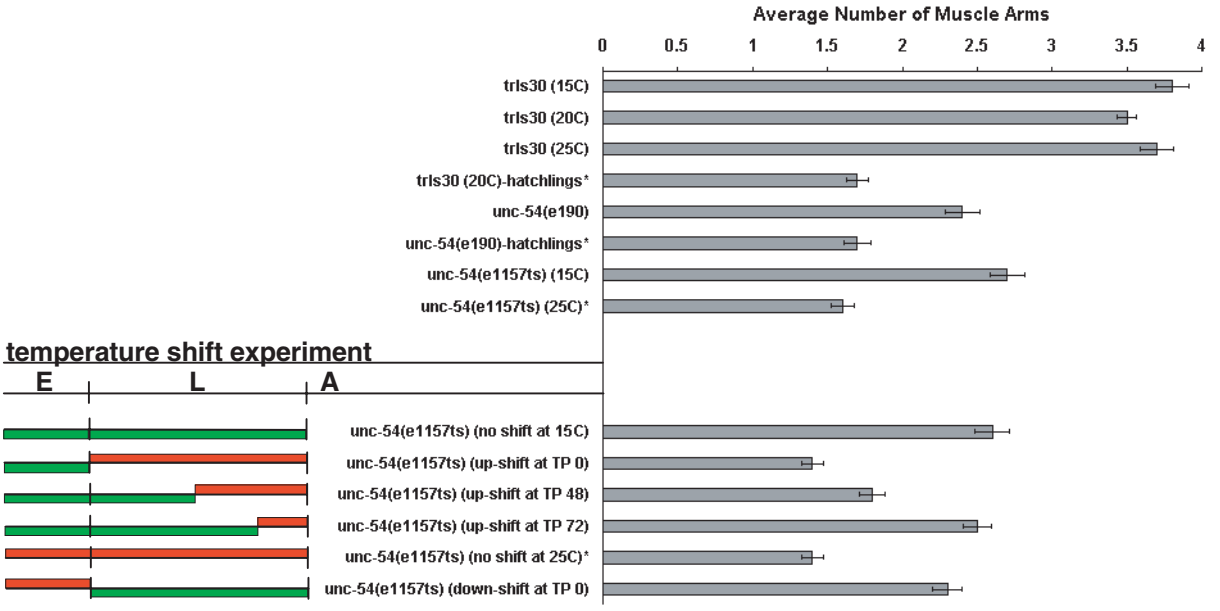

Fig. 8. Temperature shift experiments with the temperature-sensitive *unc-54(e1157)* allele. Shown is the average number of muscle arms extended by muscles 9 through 19 for the indicated genotypes. Counts for genotypes marked with an asterisk represent the average for muscles 9 to 15. For each muscle n=15, except for *trIs30* (20°C) and *trIs30* (20°C) hatchlings, for which n=30. The allele name is followed by either the temperature at which the animals were constitutively raised or a description of the time point (TP) (in hours) at which the animals were shifted to a different temperature. The coloured bars on the left represent the temperature at which animals were incubated during the indicated developmental times. Green, incubated at 15°C; red, incubated at 25°C; E, embryogenesis; L, larval development; A, adulthood. The error bars represents the standard error of the mean. Averages less than two arms per BWM are all significantly different than averages greater than two (P<0.001).

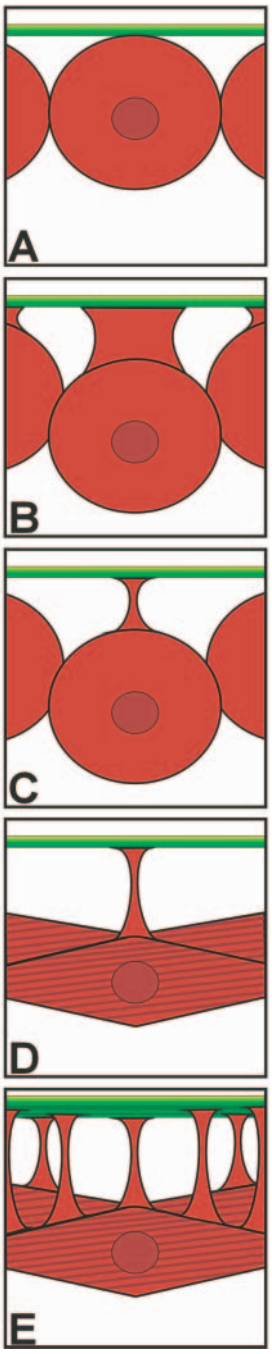

Fig. 9. A two-phase model of muscle arm development. (A) Three myoblasts (red), which juxtapose a motoneuron (green) during mid-embryogenesis. The nucleus of the centre myoblast is shown. (B) Myoblasts either migrate away or are displaced from the motoneuron, leaving a muscle arm membrane attachment behind. This is the first phase of muscle arm development. (C) The activity of *unc-54*/MHC-B and *lev-11*/tropomyosin are required to modify the morphology of the embryonic muscle arm. (D) The myoblasts complete differentiation, including the obliquely arranged sarcomeres (dark red lines represent anisotropic bands). (E) After embryogenesis and early in larval development, post-embryonic neurons develop (additional green lines). These additional axons may induce larval muscle arm extension through the secretion of a chemotropic cue. This is the second phase of muscle arm development and is dependant on actin, *unc-54*/MHC-B, *lev-11*/tropomyosin and the F-actin depolymerization activity of *unc-60B*/ADF/cofilin.

background or the RNAi-sensitive background, *rrf-3(pk1426)* (data not shown). We then examined *myo-3(st386)* animals that were mosaic for a *myo-3p*::MHC-A::GFP rescuing extra-chromosomal array *stEx30* (Campagnola et al., 2002). The number of muscle arms extended by muscles expressing MHC-A::GFP was not significantly different from muscles without MHC-A ($P>0.01$; Fig. 7). In addition, there is no significant difference in the arm widths of muscles with or without MHC-A ($P>0.01$). Together, these results strongly suggest that the muscle arm defects observed in *unc-54* mutants are not a secondary consequence of disrupted thick filaments. We conclude that muscle myosin heavy chain B is specifically required for muscle arm development.

We next determined when MHC-B is required for muscle arm development. The number of muscle arms in *unc-54(e190)* hatchlings is indistinguishable from wild-type hatchlings (Table 2, line 21), suggesting that the role of MHC-B in muscle arm extension is restricted to post-embryonic development. We then used a temperature-sensitive allele of *unc-54(e1157)* to determine when MHC-B is required for larval arm outgrowth. We found that MHC-B is required for muscle arm extension during early larval development and is coincidental with the period of muscle arm extension in wild-type larvae (Fig. 8).

unc-54(e190) mutants resembled *lev-11(RNAi)*-treated animals: the number of muscle arms was significantly reduced, the width of the remaining arms was significantly increased, the arm termini were infrequently arborized, and the BWMs did not display lateral flowing ends or membrane extension defects (Table 3). If MHC-B and LEV-11 regulate the same process, then *lev-11(RNAi)*-treated *unc-54(e190)* nulls should not have fewer muscle arms than *lev-11(RNAi)*-treated worms alone. Consistent with this hypothesis we found that *unc-54(e190); lev-11(RNAi)* animals had equivalent numbers of muscle arms to *lev-11(RNAi)* animals (Table 2, line 28). Furthermore, muscle arm widths of *unc-54(e190); lev-11(RNAi)* animals were not significantly different from those of *lev-11(RNAi)* animals and were not additive ($P>0.05$). This suggests that MHC-B and LEV-11 function together to regulate muscle arm extension and morphology.

Strikingly, *unc-54(RNAi)* enhanced the arm termini arborization phenotype in both *act-1,2,3(st15)* and *unc-60(su158)* mutants (Fig. 5, Table 3). This enhancement was both quantitative and qualitative, as the arborization was continuous from muscle to muscle in almost all *act-1,2,3(st15); unc-54(RNAi)* animals and in some *unc-60(su158)*; *unc-54(RNAi)* animals. It is intriguing that these animals also had defasciculated nerve cords. Because *unc-54* and *unc-60B* are specifically expressed in muscle and not neurons (Ardizzi and Epstein, 1987; Okkema et al., 1993; Ono et al., 1999), our results suggest that the arborization of muscle arms can lead to nerve cord defasciculation. In addition, the enhancement of arm arborization by *unc-54(RNAi)* suggests that MHC-B normally restricts actin-based membrane extension in the muscle arm termini.

Discussion

Our study provides a detailed description of muscle arm development in *C. elegans* and extends the pioneering work by others (Hall and Hedgecock, 1991; Hedgecock et al., 1990). At hatching, each BWM is connected to the nearest nerve cord by one or two muscle arms. The number of muscle arms is approximately doubled during the first larval stage, coincident with the birth of post-embryonic motoneurons. Each BWM is observed to extend a characteristic number of arms, and in many cases these arms emerge from the same location on the BWM and adopt a similar shape. Our work establishes muscle arm extension as a useful in vivo model of membrane extension because we show that muscle arm development relies on many of the same proteins that remodel the actin cytoskeleton in other systems.

A ‘two-phase’ model of muscle arm development

Adults that have null mutations in *unc-60B*/ADF/cofilin or

unc-54/MHC-B, or have been treated with *lev-11*/tropomyosin*(RNAi)*, have similar numbers of arms to wild-type hatchlings. It is unlikely that these genes have redundant functions in arm extension because various double mutant combinations fail to further reduce the number of muscle arms. Rather, we propose a 'two-phase' model of muscle arm development in which larval muscle arms develop by a fundamentally different mechanism from embryonic muscle arms (Fig. 9). Previous studies have shown that myoblast progenitors of the head and neck BWMs are born juxtaposed to the nerve ring. As embryonic development proceeds, these myoblasts move away from the nerve ring and leave muscle arms behind (C. R. Norris, I. A. Bazykina, E. M. Hedgecock, D. H. Hall, personal communication). As none of the cytoskeletal mutants we examined had fewer arms than hatchlings, we infer that all BWMs passively leave membrane connections behind as they move away from the nerve cords during embryogenesis (Phase I). We propose that BWMs actively extend muscle arms only during larval development (Phase II). Our model is supported by two additional observations. First, *unc-54*/MHC-B is required only for the extension of larval muscle arms, as *unc-54* mutant hatchlings have the same number of arms as wild-type hatchling controls. Second, the number of muscle arms in *unc-104* mutant adults is similar to wild-type hatchlings. Because UNC-104 is required to transport vesicles that probably carry the putative chemotropic cue, the remaining muscle arms in the *unc-104* mutants must not rely this cue for their development.

A novel role for muscle myosin in membrane extension

We have discovered unexpected roles for myosin heavy chain B (*unc-54*) in both phases of muscle arm development. First, MHC-B is required to regulate embryonic muscle arm morphology, as *unc-54* mutations result in a wide arm phenotype. The same phenotype is observed in *lev-11(RNAi)*-treated animals. Furthermore, *lev-11(RNAi)*-treated *unc-54* nulls do not have wider arms than either single gene disruption alone. These results suggest that MHC-B and tropomyosin act together to regulate muscle arm morphology and are consistent with the known role of tropomyosin in mediating myosin-actin interactions in both muscle and non-muscle cells (Bryce et al., 2003; Gordon et al., 2000).

In our two-phase model of arm development, embryonic muscle arms are the trailing edge remnants of myoblast movement away from the motor axons. Intriguingly, inhibition of non-muscle myosin II activity in migratory neutrophils results in a failure to retract the trailing edge, which consequently expands in size and accumulates actin filaments (Eddy et al., 2000). It has been proposed that non-muscle myosin II generates tension within the cytoskeleton of the trailing edge and promotes dissociation of adhesion complexes from the substrate, allowing forward cell translocation (Eddy et al., 2000). We similarly propose that MHC-B, which is a muscle myosin II family member (Hodge and Cope, 2000; Sellers, 2000), also generates actin-filament tension within the developing embryonic muscle arms to restrict arm width. Our model is supported by the observations that disruption of *unc-54* results in the expansion of embryonic muscle arms, the accumulation of actin within the arm terminus, and the dramatic enhancement of the actin-based arborization of termini in *unc-60B* and *act-1,2,3* mutants.

MHC-B is also required for the active extension of muscle arms during the second phase of muscle arm development. The number of muscle arms in *unc-54* null hatchlings is identical to wild-type hatchlings. Similarly, adult animals in which *unc-54* was compromised during early larval development using a temperature-sensitive allele have a similar number of muscle arms as wild-type hatchlings. These results demonstrate that MHC-B is essential for larval muscle arm extension. This is the first evidence that the muscle myosin II MHC-B can play an active role in membrane extension. However, non-muscle myosin II is well known to be required for membrane extension in many cell types (Diefenbach et al., 2002; Wylie et al., 1998; Lo et al., 2004; Pollard and Borisy, 2003). We speculate that *unc-54* mutants fail to extend larval arms because MHC-B is needed to generate the actin-based tension required for membrane extension at the leading edge as previously described in other systems (Diefenbach et al., 2002). Our observation that *unc-54(RNAi)* and *lev-11(RNAi)*-treatments can suppress the lateral flowing BWM ends and membrane extension phenotypes seen in the actin gain-of-function mutant further supports this model.

The regulation of actin dynamics during larval muscle arm extension

UNC-60B/ADF/cofilin has two important biochemical activities required for the proper assembly and maintenance of the *C. elegans* sarcomere: F-actin depolymerization and severing (Ono et al., 1999). Although all the *unc-60B* alleles that we examined disrupt sarcomere development, only those alleles that inhibit the depolymerizing activity of UNC-60B have larval muscle arm extension defects. This suggests that it is the F-actin depolymerizing activity of UNC-60B/ADF/cofilin, and not the severing activity, that is crucial to membrane extension in muscle. These observations contradict a previous report that only the severing activity of ADF/cofilin is required for membrane extension in transgenic chick neurons (Endo et al., 2003). Although both studies rely on previous biochemical analysis of mutant ADF/cofilin activity, it is possible that the mutations behave differently in vivo, or have neomorphic activities that were not considered. Alternatively, chick cofilin and *C. elegans* UNC-60B may have either divergent properties or are regulated differently in neurons or muscle cells. In any case, our results suggest that enzymatic modulation of the actin cytoskeleton is crucial for muscle arm extension.

In summary, we have demonstrated that muscle arms are a useful model system to study the mechanics of membrane extension because they are readily observed in living animals and are amenable to genetic disruption. Indeed, this work has led to novel insights into the functions of conserved cytoskeletal components and regulators. We anticipate that the study of muscle arms in *C. elegans* will be valuable in uncovering new genes required for membrane extension and guided migration.

We thank Zhibin Lu, Raynah Fernandes, and Nicole Ricker for technical assistance; Jean-Louis Bessereau for bringing the *him-4* promoter to our attention; David Hall for sharing unpublished results; Shoichiro Ono for the *lev-11* RNAi clones and *unc-60* alleles;

Geraldine Seydoux for the construct encoding the GFP::ACT-1 fusion protein; Andrew Fire for vectors; and Andrew Spence for use of his equipment and many helpful discussions. We thank Brent Derry, Joe Culotti and James Craigie for comments on the manuscript. We would also like to express our gratitude to Theresa Stiernagle and the *C. elegans* Genetic Center, which is funded by the NIH National Center for Research Resources (NCRR), for sending us many worm strains. S.J.D. is supported by a Natural Sciences and Engineering Council of Canada doctoral fellowship. P.J.R. is a Canadian Research Chair in Molecular Neurobiology. This work was supported by a Terry Fox Foundation National Cancer Institute of Canada operating grant, a Terry Fox Foundation equipment grant, and infrastructure awards from the Canadian Foundation for Innovation and Ontario Innovation Trust.

Supplementary material

Supplementary material for this article is available at
http://dev.biologists.org/cgi/content/full/132/13/3079/DC1

References

Ardizzi, J. P. and Epstein, H. F. (1987). Immunochemical localization of myosin heavy chain isoforms and paramyosin in developmentally and structurally diverse muscle cell types of the nematode *Caenorhabditis elegans*. *J. Cell Biol.* **105**, 2763-2770.

Bernstein, B. W. and Bamburg, J. R. (1982). Tropomyosin binding to F-actin protects the F-actin from disassembly by brain actin-depolymerizing factor (ADF). *Cell Motil.* **2**, 1-8.

Blanchoin, L., Amann, K. J., Higgs, H. N., Marchand, J. B., Kaiser, D. A. and Pollard, T. D. (2000). Direct observation of dendritic actin filament networks nucleated by Arp2/3 complex and WASP/Scar proteins. *Nature* **404**, 1007-1011.

Brundage, L., Avery, L., Katz, A., Kim, U. J., Mendel, J. E., Sternberg, P. W. and Simon, M. I. (1996). Mutations in a C. elegans Gqalpha gene disrupt movement, egg laying, and viability. *Neuron* **16**, 999-1009.

Bryce, N. S., Schevzov, G., Ferguson, V., Percival, J. M., Lin, J. J., Matsumura, F., Bamburg, J. R., Jeffrey, P. L., Hardeman, E. C., Gunning, P. et al. (2003). Specification of actin filament function and molecular composition by tropomyosin isoforms. *Mol. Biol. Cell* **14**, 1002-1016.

Campagnola, P. J., Millard, A. C., Terasaki, M., Hoppe, P. E., Malone, C. J. and Mohler, W. A. (2002). Three-dimensional high-resolution second-harmonic generation imaging of endogenous structural proteins in biological tissues. *Biophys. J.* **82**, 493-508.

DesMarais, V., Ichetovkin, I., Condeelis, J. and Hitchcock-DeGregori, S. E. (2002). Spatial regulation of actin dynamics: a tropomyosin-free, actin-rich compartment at the leading edge. *J. Cell Sci.* **115**, 4649-4660.

DesMarais, V., Macaluso, F., Condeelis, J. and Bailly, M. (2004). Synergistic interaction between the Arp2/3 complex and cofilin drives stimulated lamellipod extension. *J. Cell Sci.* **117**, 3499-3510.

Diefenbach, T. J., Latham, V. M., Yimlamai, D., Liu, C. A., Herman, I. M. and Jay, D. G. (2002). Myosin 1c and myosin IIB serve opposing roles in lamellipodial dynamics of the neuronal growth cone. *J. Cell Biol.* **158**, 1207-1217.

Eddy, R. J., Pierini, L. M., Matsumura, F. and Maxfield, F. R. (2000). Ca^{2+}-dependent myosin II activation is required for uropod retraction during neutrophil migration. *J. Cell Sci.* **113**, 1287-1298.

Endo, M., Ohashi, K., Sasaki, Y., Goshima, Y., Niwa, R., Uemura, T. and Mizuno, K. (2003). Control of growth cone motility and morphology by LIM kinase and Slingshot via phosphorylation and dephosphorylation of cofilin. *J. Neurosci.* **23**, 2527-2537.

Fischer, M., Kaech, S., Knutti, D. and Matus, A. (1998). Rapid actin-based plasticity in dendritic spines. *Neuron* **20**, 847-854.

Francis, G. R. and Waterston, R. H. (1985). Muscle organization in Caenorhabditis elegans: localization of proteins implicated in thin filament attachment and I-band organization. *J. Cell Biol.* **101**, 1532-1549.

Gettner, S. N., Kenyon, C. and Reichardt, L. F. (1995). Characterization of beta pat-3 heterodimers, a family of essential integrin receptors in C. elegans. *J. Cell Biol.* **129**, 1127-1141.

Ghosh, M., Song, X., Mouneimne, G., Sidani, M., Lawrence, D. S. and Condeelis, J. S. (2004). Cofilin promotes actin polymerization and defines the direction of cell motility. *Science* **304**, 743-746.

Gordon, A. M., Homsher, E. and Regnier, M. (2000). Regulation of contraction in striated muscle. *Physiol. Rev.* **80**, 853-924.

Hall, D. H. and Hedgecock, E. M. (1991). Kinesin-related gene unc-104 is required for axonal transport of synaptic vesicles in C. elegans. *Cell* **65**, 837-847.

Hedgecock, E. M., Culotti, J. G. and Hall, D. H. (1990). The unc-5, unc-6, and unc-40 genes guide circumferential migrations of pioneer axons and mesodermal cells on the epidermis in C. elegans. *Neuron* **4**, 61-85.

Hodge, T. and Cope, M. J. (2000). A myosin family tree. *J. Cell Sci.* **113**, 3353-3354.

Ichetovkin, I., Grant, W. and Condeelis, J. (2002). Cofilin produces newly polymerized actin filaments that are preferred for dendritic nucleation by the Arp2/3 complex. *Curr. Biol.* **12**, 79-84.

Jacinto, A., Wood, W., Woolner, S., Hiley, C., Turner, L., Wilson, C., Martinez-Arias, A. and Martin, P. (2002). Dynamic analysis of actin cable function during Drosophila dorsal closure. *Curr. Biol.* **12**, 1245-1250.

Kagawa, H., Gengyo, K., McLachlan, A. D., Brenner, S. and Karn, J. (1989). Paramyosin gene (unc-15) of Caenorhabditis elegans. Molecular cloning, nucleotide sequence and models for thick filament structure. *J. Mol. Biol.* **207**, 311-333.

Kagawa, H., Sugimoto, K., Matsumoto, H., Inoue, T., Imadzu, H., Takuwa, K. and Sakube, Y. (1995). Genome structure, mapping and expression of the tropomyosin gene tmy-1 of Caenorhabditis elegans. *J. Mol. Biol.* **251**, 603-613.

Kimble, J. and Hirsh, D. (1979). The postembryonic cell lineages of the hermaphrodite and male gonads in Caenorhabditis elegans. *Dev. Biol.* **70**, 396-417.

Landel, C. P., Krause, M., Waterston, R. H. and Hirsh, D. (1984). DNA rearrangements of the actin gene cluster in Caenorhabditis elegans accompany reversion of three muscle mutants. *J. Mol. Biol.* **180**, 497-513.

Lewis, J. A. and Fleming, J. T. (1995). Basic Culture Methods. In *Caenorhabditis elegans: Modern Biological Analysis of an Organism*, vol. 48 (ed. H. F. S. D. C. Epstein). San Diego, CA: Academic Press.

Lo, C. M., Buxton, D. B., Chua, G. C., Dembo, M., Adelstein, R. S. and Wang, Y. L. (2004). Nonmuscle myosin IIb is involved in the guidance of fibroblast migration. *Mol. Biol. Cell* **15**, 982-989.

Maciver, S. K. and Hussey, P. J. (2002). The ADF/cofilin family: actin-remodeling proteins. *Genome Biol.* **3**, reviews 3007.

MacLeod, A. R., Waterston, R. H., Fishpool, R. M. and Brenner, S. (1977). Identification of the structural gene for a myosin heavy-chain in Caenorhabditis elegans. *J. Mol. Biol.* **114**, 133-140.

McKim, K. S., Matheson, C., Marra, M. A., Wakarchuk, M. F. and Baillie, D. L. (1994). The Caenorhabditis elegans unc-60 gene encodes proteins homologous to a family of actin-binding proteins. *Mol. Gen Genet.* **242**, 346-357.

Mello, C. C., Kramer, J. M., Stinchcomb, D. and Ambros, V. (1991). Efficient gene transfer in C.elegans: extrachromosomal maintenance and integration of transforming sequences. *EMBO J.* **10**, 3959-3970.

Miller, D. M., Stockdale, F. E. and Karn, J. (1986). Immunological identification of the genes encoding the four myosin heavy chain isoforms of Caenorhabditis elegans. *Proc. Natl. Acad. Sci. USA* **83**, 2305-2309.

Misgeld, T., Burgess, R. W., Lewis, R. M., Cunningham, J. M., Lichtman, J. W. and Sanes, J. R. (2002). Roles of neurotransmitter in synapse formation: development of neuromuscular junctions lacking choline acetyltransferase. *Neuron* **36**, 635-648.

Mitani, S. (1995). Genetic regulation of mec-3 gene expression implicated in the specification of the mechanosensory neuron cell types in *Caenorhaabditis elegans*. *Dev. Growth Differ.* **37**, 551-557.

Mohri, K. and Ono, S. (2003). Actin filament disassembling activity of Caenorhabditis elegans actin-interacting protein 1 (UNC-78) is dependent on filament binding by a specific ADF/cofilin isoform. *J. Cell Sci.* **116**, 4107-4118.

Okkema, P. G., Harrison, S. W., Plunger, V., Aryana, A. and Fire, A. (1993). Sequence requirements for myosin gene expression and regulation in Caenorhabditis elegans. *Genetics* **135**, 385-404.

Ono, K., Parast, M., Alberico, C., Benian, G. M. and Ono, S. (2003). Specific requirement for two ADF/cofilin isoforms in distinct actin-dependent processes in Caenorhabditis elegans. *J. Cell Sci.* **116**, 2073-2085.

Ono, S. and Ono, K. (2002). Tropomyosin inhibits ADF/cofilin-dependent actin filament dynamics. *J. Cell Biol.* **156**, 1065-1076.

Ono, S., Baillie, D. L. and Benian, G. M. (1999). UNC-60B, an ADF/cofilin family protein, is required for proper assembly of actin into myofibrils in *Caenorhabditis elegans* body wall muscle. *J. Cell Biol.* **145**, 491-502.

Ono, S., McGough, A., Pope, B. J., Tolbert, V. T., Bui, A., Pohl, J., Benian,

G. M., Gernert, K. M. and Weeds, A. G. (2001). The C-terminal tail of UNC-60B (actin depolymerizing factor/cofilin) is critical for maintaining its stable association with F-actin and is implicated in the second actin-binding site. *J. Biol. Chem.* **276**, 5952-5958.

Ono, S., Mohri, K. and Ono, K. (2004). Microscopic evidence that actin-interacting protein 1 actively disassembles actin-depolymerizing factor/Cofilin-bound actin filaments. *J. Biol. Chem.* **279**, 14207-14212.

Pollard, T. D. and Borisy, G. G. (2003). Cellular motility driven by assembly and disassembly of actin filaments. *Cell* **112**, 453-465.

Ritzenthaler, S., Suzuki, E. and Chiba, A. (2000). Postsynaptic filopodia in muscle cells interact with innervating motoneuron axons. *Nat. Neurosci.* **3**, 1012-1017.

Schachat, F. H., Harris, H. E. and Epstein, H. F. (1977). Two homogeneous myosins in body-wall muscle of *Caenorhabditis elegans*. *Cell* **10**, 721-728.

Sellers, J. R. (2000). Myosins: a diverse superfamily. *Biochim. Biophys. Acta* **1496**, 3-22.

Stretton, A. O. (1976). Anatomy and development of the somatic musculature of the nematode Ascaris. *J. Exp. Biol.* **64**, 773-788.

Sulston, J. E. and Horvitz, H. R. (1977). Post-embryonic cell lineages of the nematode, *Caenorhabditis elegans*. *Dev. Biol.* **56**, 110-156.

Sulston, J. E. and Horvitz, H. R. (1981). Abnormal cell lineages in mutants of the nematode Caenorhabditis elegans. *Dev. Biol.* **82**, 41-55.

Sulston, J. E., Schierenberg, E., White, J. G. and Thomson, J. N. (1983). The embryonic cell lineage of the nematode Caenorhabditis elegans. *Dev. Biol.* **100**, 64-119.

Svitkina, T. M., Verkhovsky, A. B., McQuade, K. M. and Borisy, G. G. (1997). Analysis of the actin-myosin II system in fish epidermal keratocytes: mechanism of cell body translocation. *J. Cell Biol.* **139**, 397-415.

Timmons, L. and Fire, A. (1998). Specific interference by ingested dsRNA. *Nature* **395**, 854.

Timmons, L., Court, D. L. and Fire, A. (2001). Ingestion of bacterially expressed dsRNAs can produce specific and potent genetic interference in Caenorhabditis elegans. *Gene* **263**, 103-112.

Uchida, K. S. and Yumura, S. (2004). Dynamics of novel feet of Dictyostelium cells during migration. *J. Cell Sci.* **117**, 1443-1455.

Uhm, C. S., Neuhuber, B., Lowe, B., Crocker, V. and Daniels, M. P. (2001). Synapse-forming axons and recombinant agrin induce microprocess formation on myotubes. *J. Neurosci.* **21**, 9678-9689.

Vogel, B. E. and Hedgecock, E. M. (2001). Hemicentin, a conserved extracellular member of the immunoglobulin superfamily, organizes epithelial and other cell attachments into oriented line-shaped junctions. *Development* **128**, 883-894.

Wang, S. and Kimble, J. (2001). The TRA-1 transcription factor binds TRA-2 to regulate sexual fates in Caenorhabditis elegans. *EMBO J.* **20**, 1363-1372.

Waterston, R. H., Fishpool, R. M. and Brenner, S. (1977). Mutants affecting paramyosin in Caenorhabditis elegans. *J. Mol. Biol.* **117**, 679-697.

Waterston, R. H., Hirsh, D. and Lane, T. R. (1984). Dominant mutations affecting muscle structure in Caenorhabditis elegans that map near the actin gene cluster. *J. Mol. Biol.* **180**, 473-496.

White, J. G., Southgate, E., Thomson, J. N. and Brenner, S. (1986). The structure of the nervous system of the nematode C. elegans. *Philos. Trans. R. Soc. London Ser. B* **314**, 1-340.

Wylie, S. R., Wu, P. J., Patel, H. and Chantler, P. D. (1998). A conventional myosin motor drives neurite outgrowth. *Proc. Natl. Acad. Sci. USA* **95**, 12967-12972.

Zhou, H. M., Brust-Mascher, I. and Scholey, J. M. (2001). Direct visualization of the movement of the monomeric axonal transport motor UNC-104 along neuronal processes in living Caenorhabditis elegans. *J. Neurosci.* **21**, 3749-3755.

Table S1. A comparison of the number of muscle arms in various mutant backgrounds from select body wall muscles of the dorsal right quadrant

	Genotype*	Description	*n*	Muscle 9†	Muscle 11	Muscle 13	Muscle 15	Muscle 17	Muscle 19	μ	*P*‡	*P*§
1	*trIs30* (15C)	Wild-type young adults	15	3.5±0.6	4.0±1.1	3.5±0.7	3.9±1.0	3.0±0.7	5.0±0.9	3.8	ns	–
2	*trIs30* (20C)	Wild-type young adults	30	3.2±0.9	3.5±0.7	3.6±0.8	4.0±0.9	2.8±0.7	4.1±0.7	3.5	–	–
3	*trIs30* (25C)	Wild-type young adults	15	3.3±0.7	3.3±0.6	3.5±0.8	3.9±0.5	3.1±0.8	5.2±1.0	3.7	ns	–
4	*trIs30(0RNAi)*	Wild-type young adults	15	3.1±0.7	3.7±0.5	3.7±0.8	3.6±0.5	2.9±0.8	4.2±0.7	3.5	ns	–
5	*trIs30* (20C)	Wild-type L1 hatchlings	30	1.3±0.5	2.1±1.1	1.6±0.6	1.7±0.7	–	–	1.7	<0.001	
6	*sma-6(e1482)*	Tgf-β receptor (small worms)	15	3.0±0.9	3.5±0.9	3.3±0.6	3.7±0.9	2.9±0.5	3.7±0.7	3.4	ns	–
7	*lon-2(e678)*	Glypican (long worms)	15	3.1±1.3	3.9±1.0	4.0±0.9	4.1±1.5	2.8±0.8	4.3±0.7	3.7	ns	–
8	*dpy-5(e61)*	Collagen (short worms)	15	3.4±0.5	3.5±0.8	3.3±0.6	3.9±0.5	–	–	3.6	ns	–
9	*dyp-10(e128)*	Collagen (control for *unc-104* null)	15	3.5±0.6	3.1±0.7	3.3±0.8	4.6±0.7	–	–	3.6	ns	–
10	*act-1,2,3(st15)*	Actin	15	2.5±1.0	2.2±1.0	2.4±1.0	2.6±0.9	–	–	2.4	<0.001	<0.001 (5)
11	*unc-60(su158)*	ADF/cofilin (null)	15	1.5±0.5	1.5±0.6	2.0±0.8	1.9±0.9	1.5±0.7	2.3±1.4	1.8	<0.001	ns (5)
12	*unc-60(e723)*	ADF/cofilin (hypomorph)	15	1.7±0.6	1.7±0.8	1.5±0.6	1.8±0.8	1.6±0.7	2.6±1.0	1.8	<0.001	ns (5)
13	*unc-60(s1307)*	ADF/cofilin (hypermorph)	15	3.0±1.1	3.3±1.1	3.3±1.0	3.5±0.6	2.8±0.8	4.2±0.8	3.3	ns	<0.001 (11)
14	*unc-60(r398)*	ADF/cofilin (no severing)	15	3.3±0.8	2.9±1.0	3.5±1.1	4.0±1.1	1.9±0.6	4.3±1.3	3.3	ns	<0.001 (11)
15	*unc-78(gk27)*	Actin-interacting protein 1	15	3.5±0.9	3.9±0.8	3.5±0.9	3.5±0.5	2.3±0.6	3.9±0.9	3.4	ns	–
16	*lev-11(TM1-RNAi)*	Tropomyosin	15	1.9±0.6	2.1±0.9	1.7±0.9	1.8±0.8	1.7±0.6	3.3±1.2	2.1	<0.001	ns (5)
17	*lev-11(TM2-RNAi)*	Tropomyosin	15	2.0±0.7	2.1±0.6	1.9±0.8	1.7±1.0	1.6±0.5	3.7±1.3	2.2	<0.001	0.038 (5)
18	*act-1,2,3(st15); lev-11(TM1-RNAi)*	–	15	1.7±0.6	1.5±0.8	1.5±0.7	2.1±1.0	–	–	1.7	<0.001	ns (16/ ns (5)
19	*unc-60(su158); lev-11(TM1-RNAi)*	–	15	1.2±0.4	1.7±0.5	1.7±0.7	1.2±0.4	–	–	1.4	<0.001	ns (11/ ns (5)
20	*unc-54(e190)*	Muscle myosin (MHC B)	15	2.0±0.8	2.0±0.9	2.1±0.8	3.0±1.0	2.3±0.8	3.2±1.4	2.4	<0.001	<0.001 (5)
21	*unc-54(e190)*	*unc-54* L1 hatchlings	15	1.6±0.6	1.4±0.5	1.8±0.6	2.1±0.8	–	–	1.7	<0.001	ns (5)
22	*unc-54(e1152)*	Muscle myosin (MHC B)	15	1.3±0.5	1.9±0.8	2.1±1.0	2.7±0.9	2.4±0.6	3.5±1.1	2.3	<0.001	–
23	*unc-54(RNAi)*	Muscle myosin (MHC B)	15	1.9±1.2	1.8±0.7	2.1±0.7	1.8±0.7	2.0±1.0	4.1±1.2	2.3	<0.001	ns (20)
24	*unc-54(e1157ts)* (15C)	Controls for time course	15	2.3±0.8	2.5±0.5	2.3±0.9	2.8±0.9	2.0±0.7	4.3±1.0	2.7	<0.001	–
25	*unc-54(e1157ts)* (20C)	Controls for time course	15	1.7±1.0	1.7±0.6	1.9±0.6	1.9±0.7	1.3±0.5	2.2±1.0	1.8	<0.001	<0.001 (24)
26	*unc-54(e1157ts)* (25C)	Controls for time course	15	1.7±0.7	1.3±0.6	1.5±0.6	1.9±0.7	–	–	1.6	<0.001	<0.001 (24)
27	*unc-54(e1157ts)* (15C to 15C at TP 0)	Up-shift time course	15	2.1±0.8	2.3±1.1	2.5±0.8	3.2±1.1	1.9±0.7	3.9±0.8	2.6	<0.001	–
28	*unc-54(e1157ts)* (15C to 25C at TP 0)	Up-shift time course	15	1.3±0.6	1.3±0.5	1.5±1.0	1.5±0.6	1.1±0.4	1.8±0.6	1.4	<0.001	<0.001 (27)
29	*unc-54(e1157ts)* (15C to 25C at TP 48)	Up-shift time course	15	1.8±0.8	1.5±0.6	1.9±0.7	1.7±0.7	1.4±0.6	2.7±0.7	1.8		
30	*unc-54(e1157ts)* (15C to 25C at TP 72)	Up-shift time course	15	2.4±0.8	2.1±0.8	2.6±0.7	2.8±0.8	1.7±0.6	3.3±0.8	2.5		
31	*unc-54(e1157ts)* (25C to 25C at TP 0)	Down-shift time course	15	1.3±0.5	1.5±0.6	1.2±0.4	1.7±0.6	–	–	1.4	<0.001	–
32	*unc-54(e1157ts)* (25C to 15C at TP 0)	Down-shift time course	15	1.7±0.7	2.3±0.8	2.6±1.0	2.6±1.0	1.5±0.6	2.9±0.9	2.3	<0.001	<0.001 (31)
33	*unc-15(e73)*¶	Paramyosin	15	2.5±0.7	2.0±0.5	2.8±0.9	3.1±1.3	2.2±1.0	3.4±1.1	2.7	<0.001	–
34	*unc-15(su2000)*¶	Paramyosin	15	2.7±0.5	2.2±0.4	2.5±0.8	3.8±1.0	2.7±0.9	3.9±0.9	3.0	<0.001	–
35	*unc-15(RNAi)*	Paramyosin	15	2.9±0.7	3.0±0.8	3.1±0.9	3.5±1.2	2.1±0.7	4.1±1.7	3.1	<0.001	0.007 (33)
36	*unc-15(e1402ts)* (25C)¶	Paramyosin	15	3.4±1.2	2.73±1.0	3.1±0.9	3.1±1.0			3.1	0.003	
37	*unc-54(e190); lev-11(TM1-RNAi)*	–	15	1.7±0.7	1.9±0.8	1.9±0.8	2.4±1.2	2.1±0.9	2.7±0.8	2.1	<0.001	–
38	*act-1,2,3(st15); unc-54(RNAi)*	–	15	2.9±0.9	2.7±1.2	2.7±1.1	3.1±1.3	–	–	2.9	<0.001	0.037 (10)
39	*unc-60(su158); unc-54(RNAi)*	–	15	1.3±0.5	1.3±0.5	1.4±0.5	1.8±0.8	1.5±1.0	2.2±1.0	1.6	<0.001	ns (11)
40	*unc-104(e1265)*	Kinesin	15	1.8±0.8	2.5±1.4	2.1±1.1	1.3±0.7	0.3±0.5	2.2±1.4	1.7	<0.001	ns (5)
41	*unc-104(rh43)*	Kinesin	15	1.2±0.9	1.5±1.1	1.6±1.0	1.0±0.7	0.6±0.6	1.8±1.1	1.3	<0.001	0.011 (5)
42	*dyp-10(e128) unc-104(rh142)*	*unc-104* null	15	1.3±0.8	1.2±0.6	1.1±0.5	1.1±0.6	–	–	1.2	<0.001	<0.001 (5)
43	*egl-30(n715)*	G protein α-subunit	15	3.2±0.9	3.4±0.9	3.5±0.8	4.6±0.8	3.1±0.7	4.6±0.9	3.7	ns	–
44	*egl-31(n472)*¶	Unknown	15	3.9±1.0	3.8±0.8	3.7±1.2	4.7±1.2	–	5.5±1.3	4.3 (all)	<0.001	–
45	*C26G2.1p::DsRed2*	Control for Mb::YFP	15	3.7±0.6	3.7±0.6	3.7±0.8	4.0±0.7	–	–	3.8	ns	

*All counts were made in the *trIs30* background, except ¶, which were carried out with a *him-4p::Mb::YFP* extra-chromosomal array. All counts are from young adults raised at 20°C, unless otherwise indicated in the description column.

†Only six muscles from the dorsal right quadrant were considered.

‡These *P* values were derived from Mann-Whitney tests with respect to the *trIs30* counts (row 2).

§These P values were derived from Mann-Whitney tests with respect to the counts from the row indicated in brackets. ns, not significant ($P>0.05$).